Accelerated High-Resolution Photoacoustic Tomography via Compressed Sensing

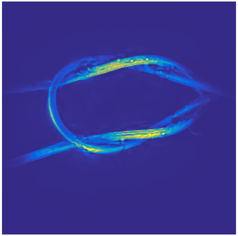
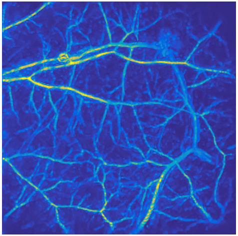
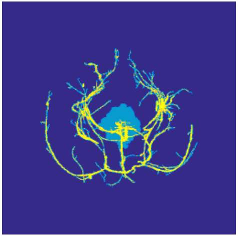

Felix Lucka
University College London
f.lucka@ulc.ac.uk

joint with:
Simon Arridge, Paul Beard, Marta Betcke,
Ben Cox, Nam Huynh & Edward Zhang

Centre for Medical Image Computing

SIAM-IS, Albuquerque,
May 24, 2016.

UCL CENTRE FOR INVERSE PROBLEMS

Optical Part

chromophore concentration: c_k

optical absorption coefficient: $\mu_a(c)$

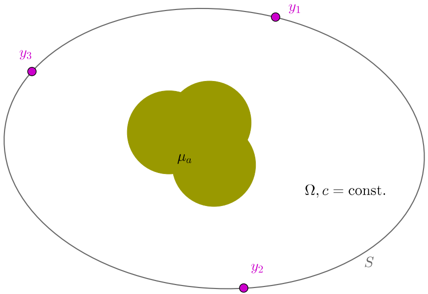

Acoustic Part

Photoacoustic Imaging: Basic Principles

Optical Part

chromophore concentration: c_k

optical absorption coefficient: $\mu_a(c)$

pulsed laser excitation: $\Phi(\mu_a)$

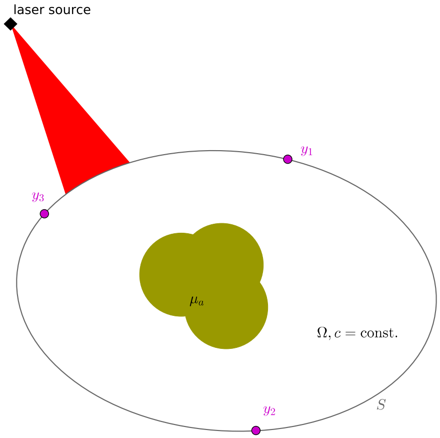

Acoustic Part

Optical Part

chromophore concentration: c_k

optical absorption coefficient: $\mu_a(c)$

pulsed laser excitation: $\Phi(\mu_a)$

thermalization: $H = \mu_a \Phi(\mu_a)$

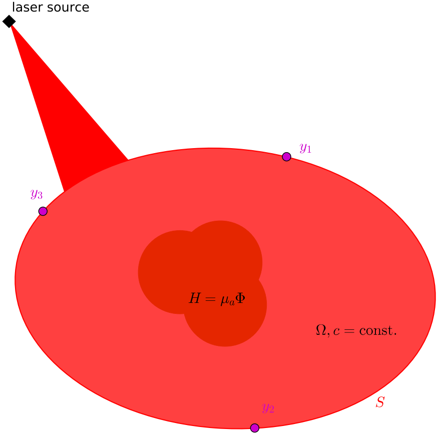

Acoustic Part

Photoacoustic Imaging: Basic Principles

Optical Part

chromophore concentration: c_k

optical absorption coefficient: $\mu_a(c)$

pulsed laser excitation: $\Phi(\mu_a)$

thermalization: $H = \mu_a \Phi(\mu_a)$

Acoustic Part

local pressure increase: $p_0 = \Gamma H$

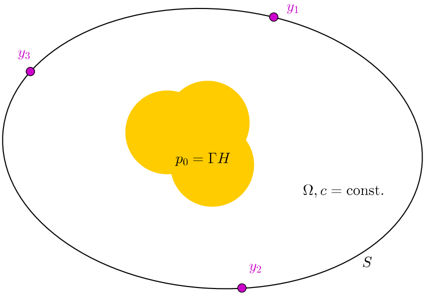

Photoacoustic Imaging: Basic Principles

Optical Part

chromophore concentration: c_k

optical absorption coefficient: $\mu_a(c)$

pulsed laser excitation: $\Phi(\mu_a)$

thermalization: $H = \mu_a \Phi(\mu_a)$

Acoustic Part

local pressure increase: $p_0 = \Gamma H$

elastic wave propagation:

$$\Delta p - \frac{1}{c^2} \frac{\partial^2 p}{\partial^2 t} = 0$$

$$p|_{t=0} = p_0, \quad \frac{\partial p}{\partial t}|_{t=0} = 0$$

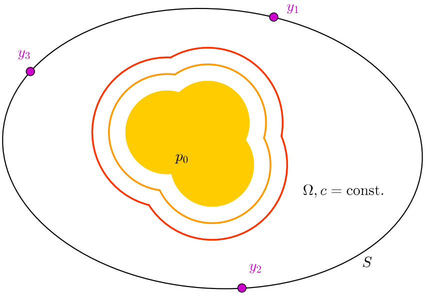

Optical Part

chromophore concentration: c_k

optical absorption coefficient: $\mu_a(c)$

pulsed laser excitation: $\Phi(\mu_a)$

thermalization: $H = \mu_a \Phi(\mu_a)$

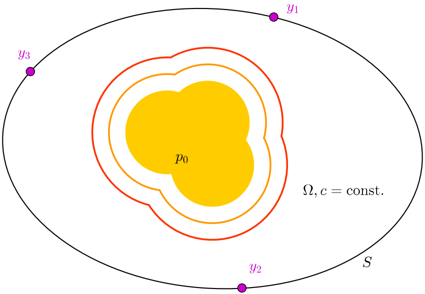

Acoustic Part

local pressure increase: $p_0 = \Gamma H$

elastic wave propagation:

$$\Delta p - \frac{1}{c^2}\frac{\partial^2 p}{\partial^2 t} = 0$$

$$p|_{t=0} = p_0, \quad \frac{\partial p}{\partial t}|_{t=0} = 0$$

measurement of pressure time courses:

$$f_i(t) = p(y_i, t)$$

Photoacoustic Imaging: Basic Principles

UCL

Optical Part

chromophore concentration: c_k

optical absorption coefficient: $\mu_a(c)$

pulsed laser excitation: $\Phi(\mu_a)$

thermalization: $H = \mu_a \Phi(\mu_a)$

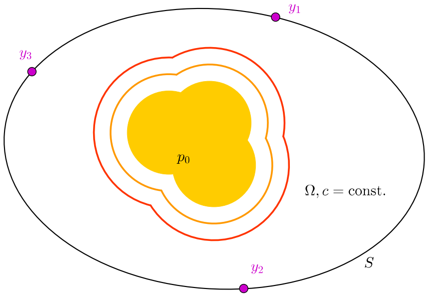

Acoustic Part

local pressure increase: $p_0 = \Gamma H$

elastic wave propagation:

$$\Delta p - \frac{1}{c^2}\frac{\partial^2 p}{\partial^2 t} = 0$$

$$p|_{t=0} = p_0, \quad \frac{\partial p}{\partial t}|_{t=0} = 0$$

measurement of pressure time courses:

$$f_i(t) = p(y_i, t)$$

Photoacoustic effect

- coupling of optical and acoustic modalities.
- "hybrid imaging"
- high optical contrast can be read by high-resolution ultrasound.

Photoacoustic Imaging: Basic Principles

UCL

Optical Part

chromophore concentration: c_k

optical absorption coefficient: $\mu_a(c)$

pulsed laser excitation: $\Phi(\mu_a)$

thermalization: $H = \mu_a \Phi(\mu_a)$

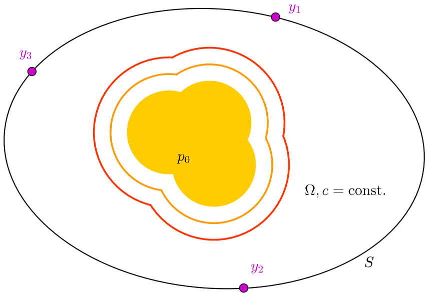

Acoustic Part

local pressure increase: $p_0 = \Gamma H$

elastic wave propagation:

$$\Delta p - \frac{1}{c^2}\frac{\partial^2 p}{\partial^2 t} = 0$$

$$p|_{t=0} = p_0, \quad \frac{\partial p}{\partial t}|_{t=0} = 0$$

measurement of pressure time courses:

$$f_i(t) = p(y_i, t)$$

Photoacoustic effect

- coupling of optical and acoustic modalities.
- "hybrid imaging"
- high optical contrast can be read by high-resolution ultrasound.

Photoacoustic Sensing Systems

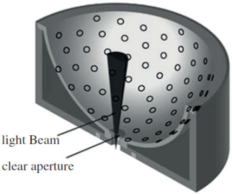

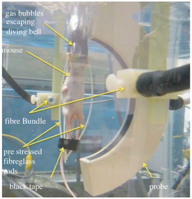

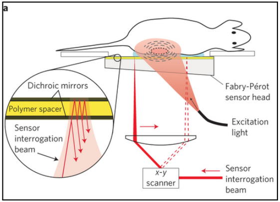

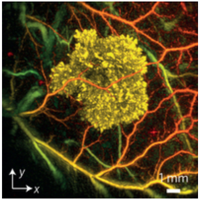

from: **Beard, 2011**, *Interface Focus*; **Jathoul et al., 2015**, *Nature Photonics*

Photoacoustic Sensing Systems

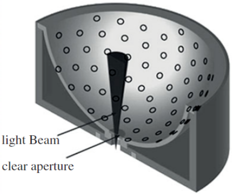

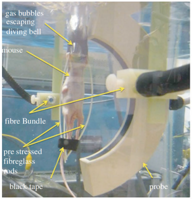

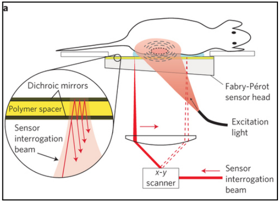

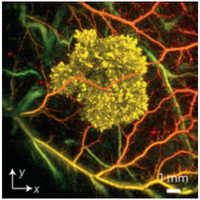

from: **Beard, 2011**, *Interface Focus*; **Jathoul et al., 2015**, *Nature Photonics*

- High res 3D PA images require sampling acoustic waves with a frequency content in the tens of MHz over cm scale apertures.
- Nyquist criterion results in tens of µm scale sampling intervals $\Longrightarrow$ several thousand detection points.
- Sequential scanning currently takes several minutes.
- Crucial limitation for clinical, spectral and dynamical PAT (4D PAT).

Photoacoustic Sensing Systems

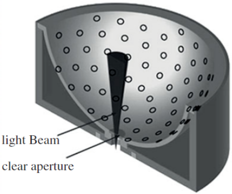

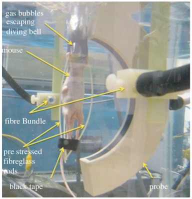

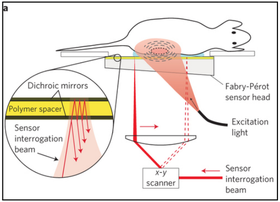

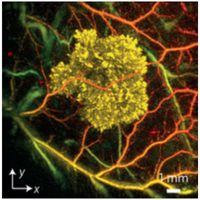

from: **Beard, 2011**, *Interface Focus*; **Jathoul et al., 2015**, *Nature Photonics*

Key observation and idea:

- Nyquist is too conservative (only band-limitlessness is assumed).
- Typical targets have additional structure, e.g., low spatial complexity (sparsity).
- Regularly sampled data is highly redundant.
- Non-redundant part could be sensed faster.
- Accelerated acquisition without significant loss of image quality.

Established as compressed sensing, successful in similar modalities.

Novel Fabry-Pérot-Based Sensing Systems

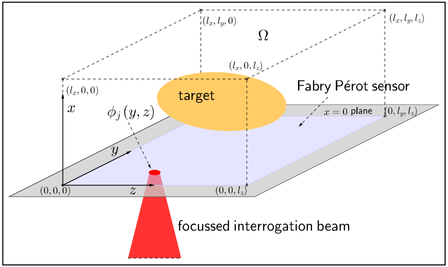

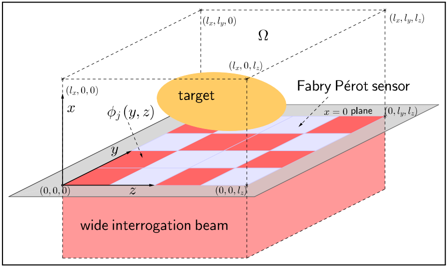

$$f_j(t) = \int p(x=0, y, z, t)\phi_j(y, z)\,\mathrm{d}y\mathrm{d}z$$

- Single-point sub-sampling (structured or random).
- Patterned interrogation similar to "single-pixel" Rice camera (via micromirror array).
- Multi-beam scanning + sub-sampling.

Applicable to other sequential scanning schemes, see **Huynh et al., 2014, 2015, 2016** for technical details.

Novel Fabry-Pérot-Based Sensing Systems

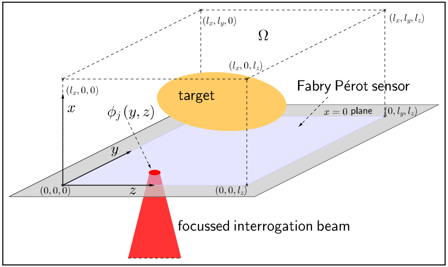

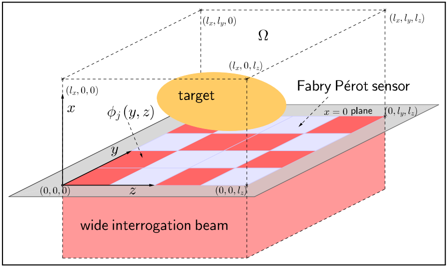

Image model: $$f_i^c = C_i f_i = C_i(Ap_i + \varepsilon_i)$$ for each frame i.

Image reconstruction:

- $f_i^c \longrightarrow f_i$, $f_i \longrightarrow p_i$ by standard method, frame-by-frame.
- $f_i^c \longrightarrow p_i$: standard or new method, frame-by-frame.
- $F^c \longrightarrow F$, $f_i \longrightarrow p_i$ by standard method, frame-by-frame.
- $F^c \longrightarrow P$: Full spatio-temporal method.

Novel Fabry-Pérot-Based Sensing Systems

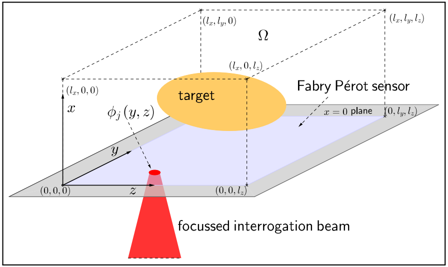

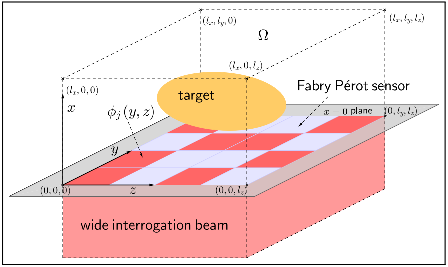

Image model: $f_i^c = C_i f_i = C_i(Ap_i + \varepsilon_i)$ for each frame i.

Image reconstruction:

- $f_i^c \longrightarrow f_i$, $f_i \longrightarrow p_i$ by standard method, frame-by-frame.
- $f_i^c \longrightarrow p_i$: standard or new method, frame-by-frame.
- $F^c \longrightarrow F$, $f_i \longrightarrow p_i$ by standard method, frame-by-frame.
- $F^c \longrightarrow P$: Full spatio-temporal method.

Standard Reconstruction & Numerical Wave Propagation

Analytic methods, e.g. eigenfunction expansion and closed-form filtered-backprojection, are too restrictive for us.

Time Reversal (TR):

- "Least restrictive PAT reconstruction"
- Sending the recorded waves "back" into volume.
- Requires a numerical model for acoustic wave propagation.

k-Wave♣ implements a *k*-space pseudospectral method to solve the underlying system of first order conservation laws:

- Compute spatial derivatives in Fourier space: 3D FFTs.
- Modify finite temporal differences by *k*-space operator and use staggered grids for accuracy and robustness.
- Perfectly matched layer to simulate free-space propagation.
- Parallel/GPU computing leads to massive speed-ups.

♣**B. Treeby and B. Cox, 2010**. *k-Wave: MATLAB toolbox for the simulation and reconstruction of photoacoustic wave fields*, *Journal of Biomedical Optics.*

A Realistic Numerical Phantom

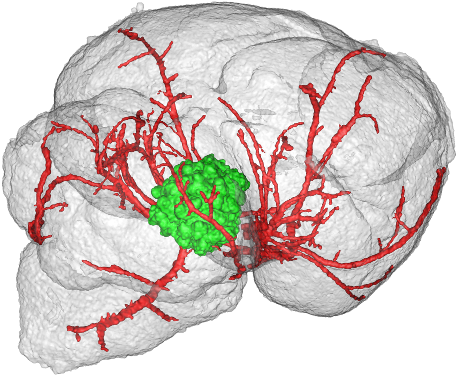

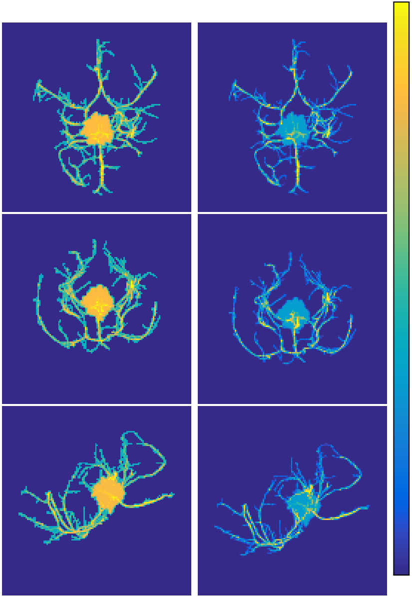

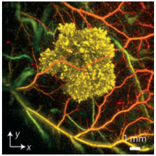

Time Reversal for Sub-Sampled Data

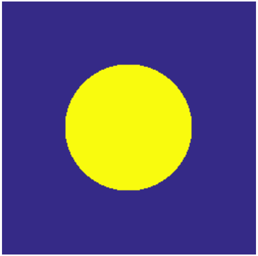

(a) IC, $n = 256^3$

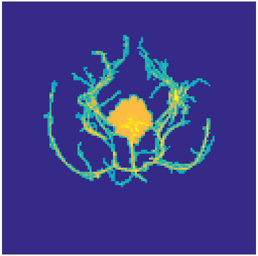

(b) high con., IC, $n = 128^3$

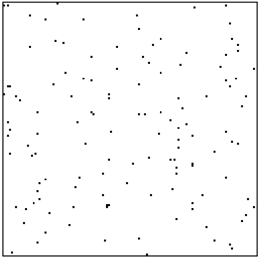

(c) sub-sampling, 128x

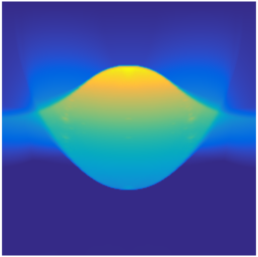

(d) TR 1

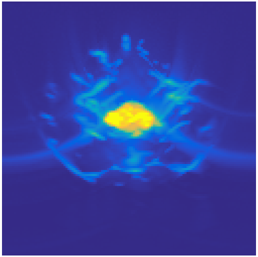

(e) TR 2

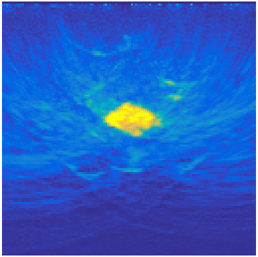

(f) TR 2, sub-sampled

sensor on top; inverse crime data sampled at Nyquist; max intensity proj., side view

Time Reversal for Sub-Sampled Data II

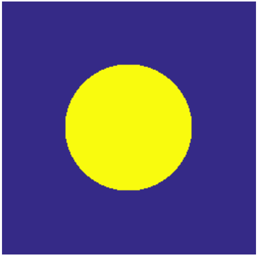

(a) IC, $n = 256^3$

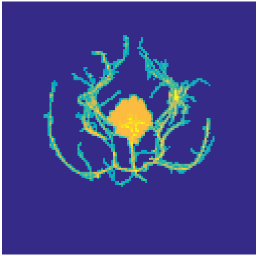

(b) high con., IC, $n = 128^3$

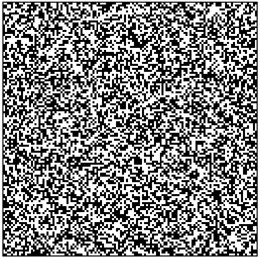

(c) sub-sampling, $1/128$

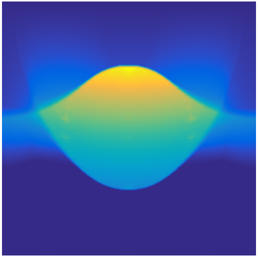

(d) TR 1

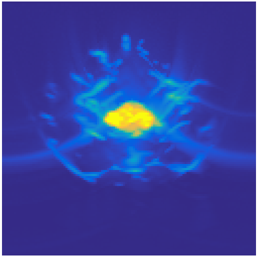

(e) TR 2

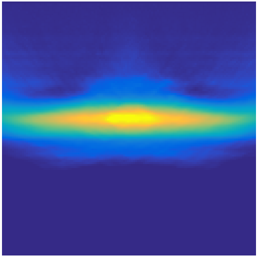

(f) TR 2, sub-sampled

sensor on top; inverse crime data sampled at Nyquist; max intensity proj., side view

Solving variational regularization problems

$$\hat{p} = \underset{p \geqslant 0}{\operatorname{argmin}} \left\{ \tfrac{1}{2} \| CAp - f^c \|_2^2 + \lambda \mathcal{J}(p) \right\}$$

iteratively by first-order methods requires implementation of A and A^*.

k-Wave yields a discrete representation A_κ. For A^*, one can

1) adjoint k-Wave iteration to obtain $(A_\kappa)^*$ (algebraic adjoint):

- ✓ high numerical accuracy.
- ! tedious derivation, specific for k-Wave, limited insights.

Huang, Wang, Nie, Wang, Anastasio, 2013. *IEEE Trans Med Imaging*

2) derive analytical adjoint and discretize it, e.g., $(A^*)_\kappa$.

- ✓ good numerical accuracy.
- ✓ simple proof, theoretical insights, generalizes to various numerical schemes.

Arridge, Betcke, Cox, L, Treeby, 2015. *On the Adjoint Operator in Photoacoustic Tomography*, (*submitted, arXiv:1602.02027*).

Comparison for Conventional Data

$$\hat{p} = \underset{p \geqslant 0}{\operatorname{argmin}} \left\{ \frac{1}{2} \| Ap - f \|_2^2 + \lambda \mathcal{J}(p) \right\}$$

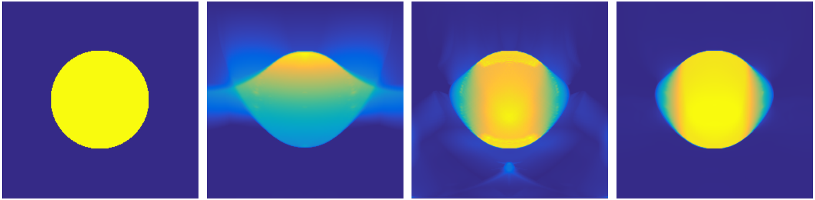

(a) $n = 256^3$ (b) TR (c) LS+ (d) TV+

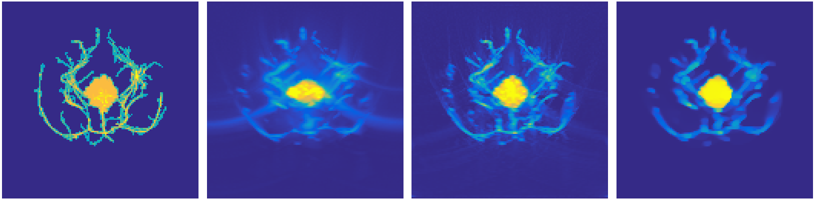

(e) $n = 128^3$ (f) TR (g) LS+ (h) TV+

sensor on top; inverse crime data sampled at Nyquist; max intensity proj., side view

Sub Sampled Data, Best Case Scenario

$$\hat{p} = \underset{p \geqslant 0}{\operatorname{argmin}} \left\{ \frac{1}{2} \| CAp - f^c \|_2^2 + \lambda \mathcal{J}(p) \right\}$$

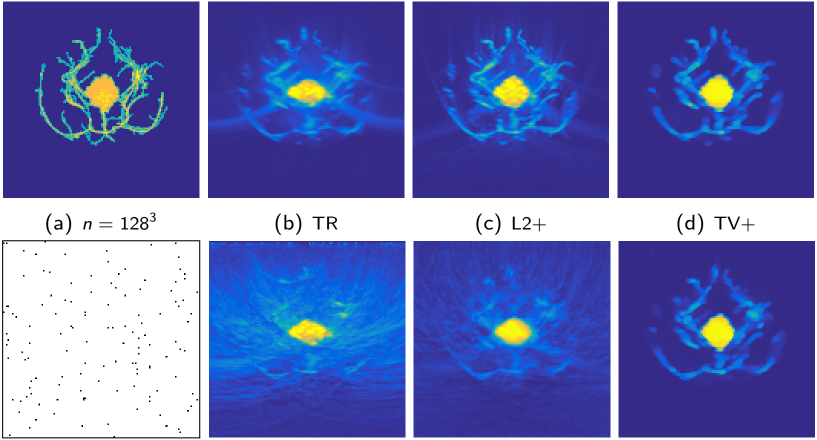

(a) $n = 128^3$ (b) TR (c) L2+ (d) TV+

(e) SubSam, 128x (f) TR (g) L2+ (h) TV+

sensor on top; inverse crime data sampled at Nyquist; max intensity proj., side view

! Data created by the same forward model used for reconstruction.

! Conventional data was sampled at Nyquist rates in space and time.

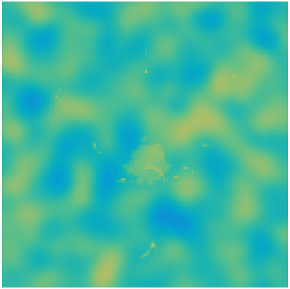

(a) $c_0 + \tilde{c}$

(b)

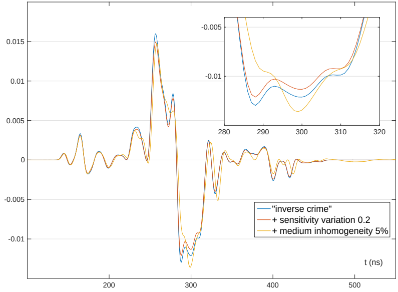

(c) pressure-time courses

To obtain more realistic results:

- Generate data with perturbed, heterogeneous acoustic model.
- Model inhomogenous sensitivity and noise level of sensor channels.
- Conventional, "full" data is acquired below spatial Nyquist rate.

Conventional data acquired on 2×2 too coarse grid.

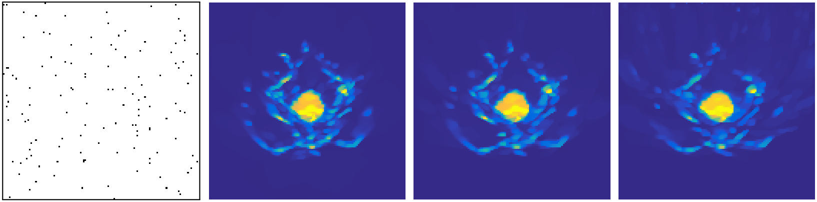

(d) single point (e) TV+Br, 1x (f) TV+Br, 8x (g) TV+Br, 32x

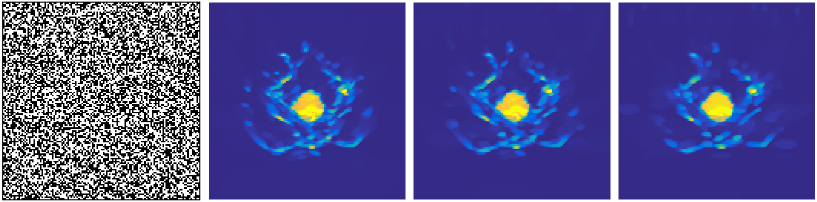

(h) patterned inter. (i) TV+Br, 1x (j) TV+Br, 8x (k) TV+Br, 32x

sensor on top; max intensity proj., side view

Leaving the Comfort Zone: Reproduction on Real Data

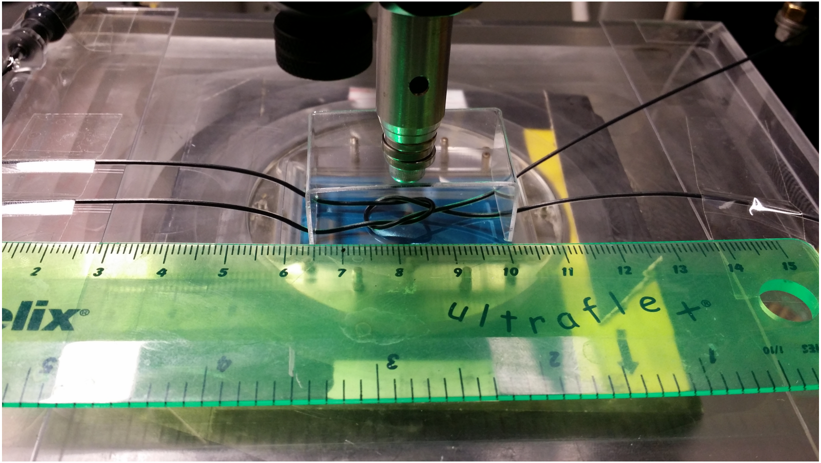

- Two polythene tubes filled with 10/100% ink.
- Stop-motion-style data acquisition of pulling one tube end.
- 45 frames (15min for conventional scanning per frame).
- Conventional data reconstructions to validate sub-sampling.

Conventional "Full" Data

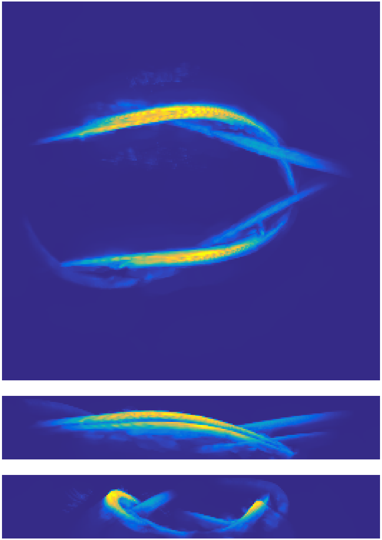

TR & TV denoising

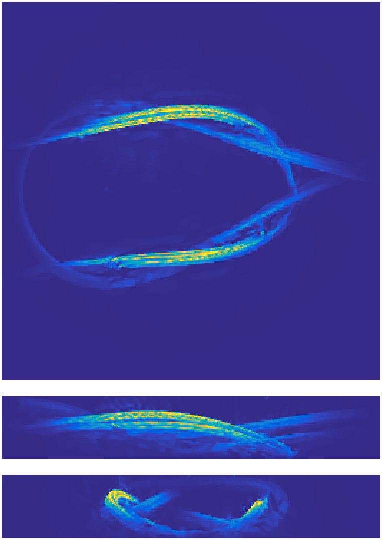

TV+

Random Point Sub-Sampled Data, 4x

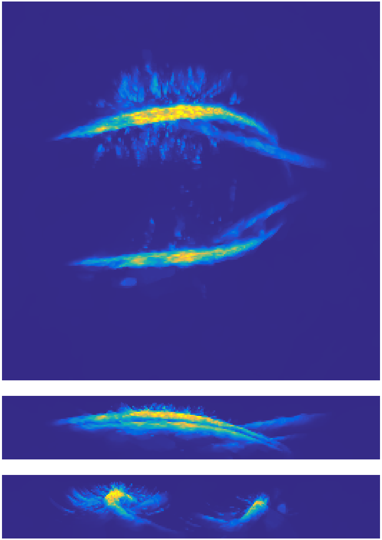

TR & TV denoising

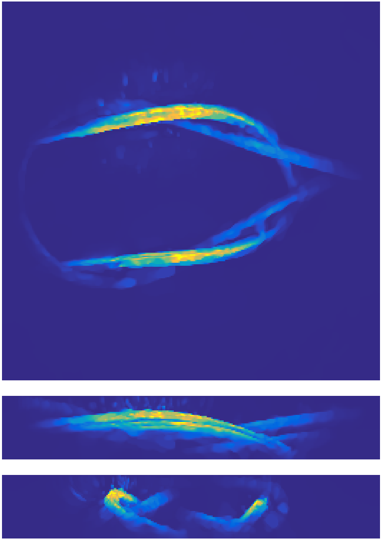

TV+

Random Point Sub-Sampled Data, 8x

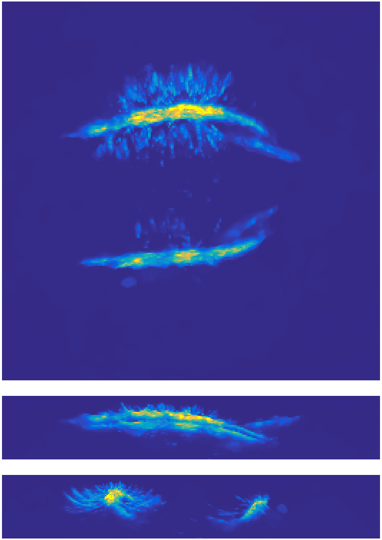

TR & TV denoising

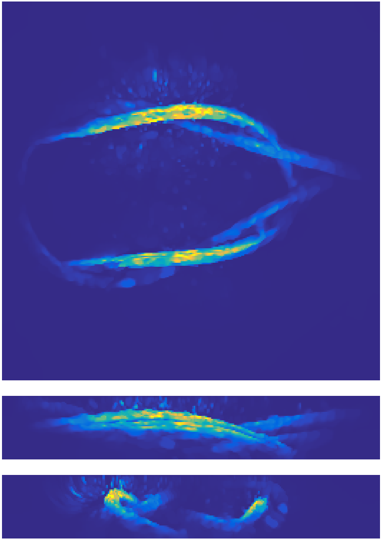

TV+

Random Point Sub-Sampled Data, 16x

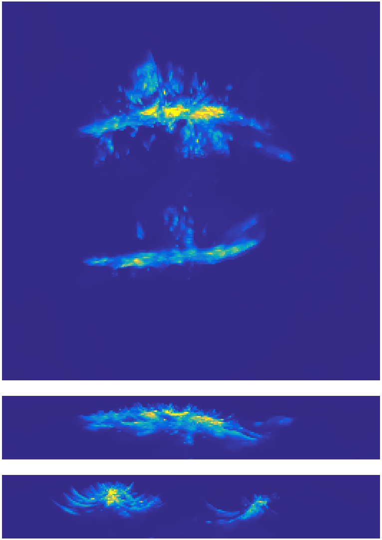

TR & TV denoising

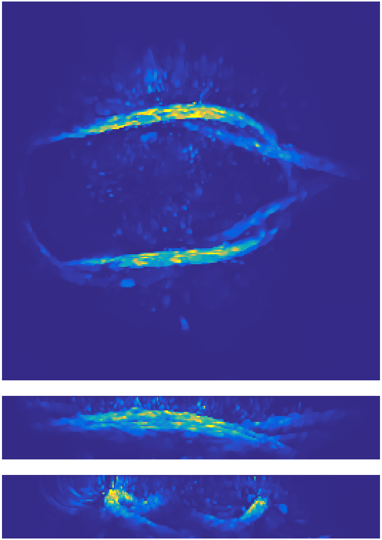

TV+

In Vivo Measurements: Conventional Data

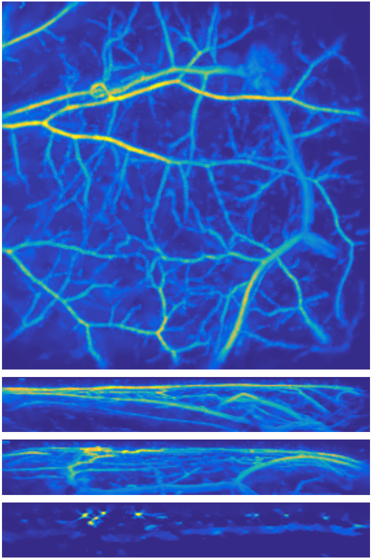

TR & TV denoising

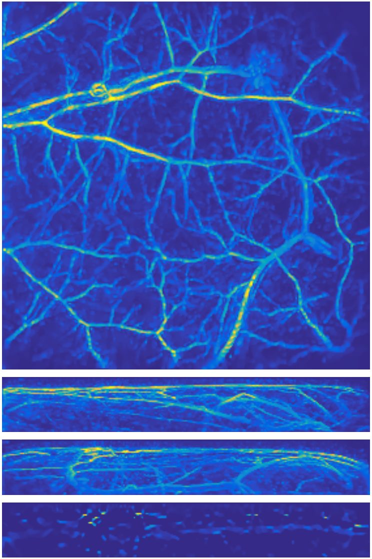

Bregman TV+

Thanks to Olumide Ogunlade for the excellent data!

In Vivo Measurements: 4x

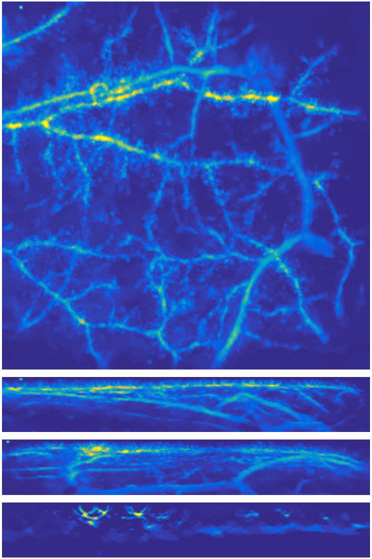

TR & TV denoising

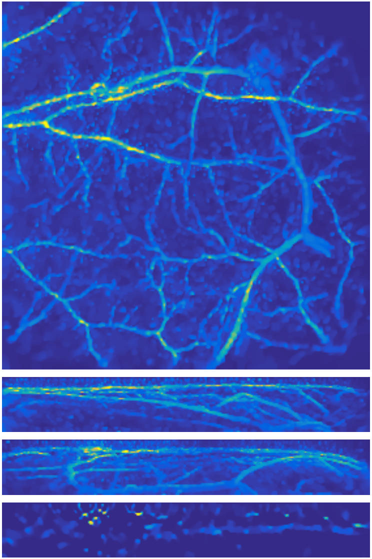

Bregman TV+

Thanks to Olumide Ogunlade for the excellent data!

In Vivo Measurements: 8x

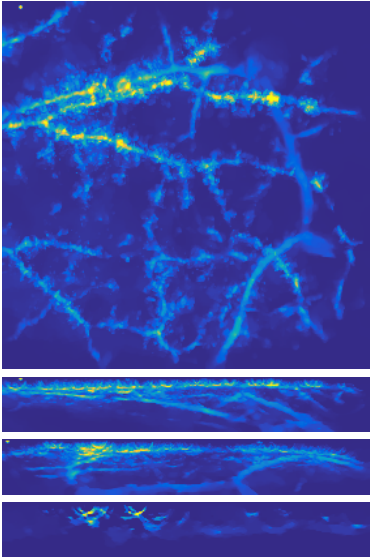

TR & TV denoising

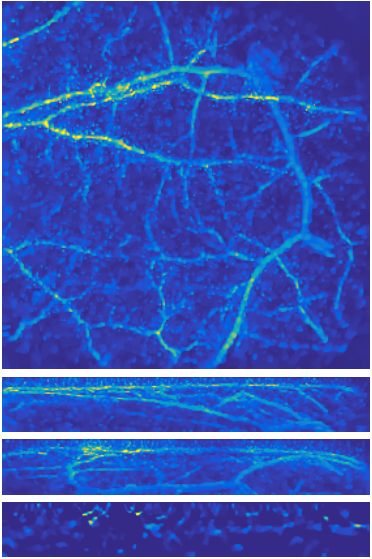

Bregman TV+

Thanks to Olumide Ogunlade for the excellent data!

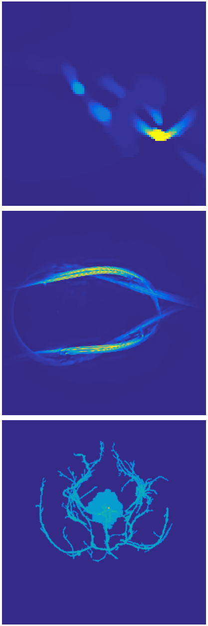

Continuous data acquisition

$\Longrightarrow$ tradeoff between spatial and temporal resolution.

Different dynamic models:

- Structured Low-Rank (functional imaging with static anatomies/QPAT).
- Tracer uptake/wash-in models.
- Perfusion models.
- Needle guidance
- Optical flow constraints for joint image reconstruction and motion estimation.

Low Rank Structures: A Very Simple Example

$$P = W \cdot V, \qquad P \in \mathbb{R}^{N\times K},\ W \in \mathbb{R}^{N\times R},\ V \in \mathbb{R}^{R\times K},\ R \leqslant \min(N, K)$$

Example, $N = 10\,000$, $K = 25$, $R = 1$:

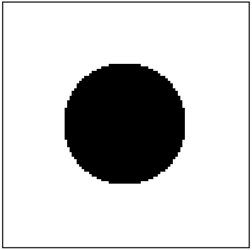

$W \in \mathbb{R}^{N\times 1}$

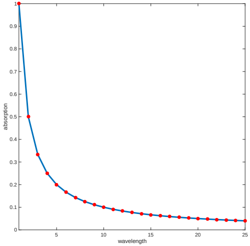

$V \in \mathbb{R}^{1\times K}$

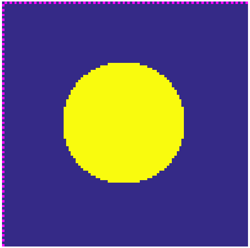

$P(\cdot, 1)$

Can we acquire multi-spectral data as fast as one conventional scan?

- spatial sub-sampling by factor $K = 25$.
- 4 instead of 100 scanning locations per wave length.
- geometric information scattered over data set.

$$\hat{p}_i = \operatorname*{argmin}_{p \geqslant 0} \left\{ \| C_i A p - f_i^c \|_2^2 \right\} \quad \forall\, i = 1, \ldots, K$$

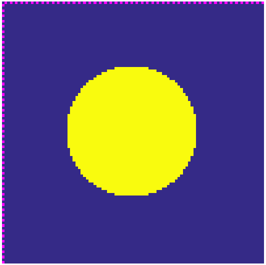

ground truth

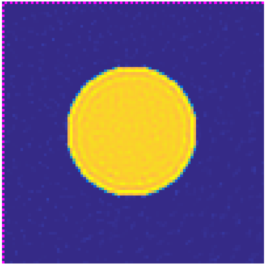

conventional data

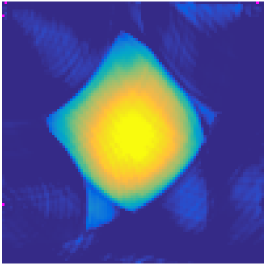

sub-sam. data

Neither geometry nor spectrum can be recovered!

Nuclear Norm Regularized Least Squares

$$\hat{P} = \underset{P \geqslant 0}{\text{argmin}} \left\{ \tfrac{1}{2} \| CAP - F^c \|_{fro}^2 + \lambda |P|_* \right\}$$

λ such that $\text{rank}(P) = 1$ + Bregman iter to restore contrast.

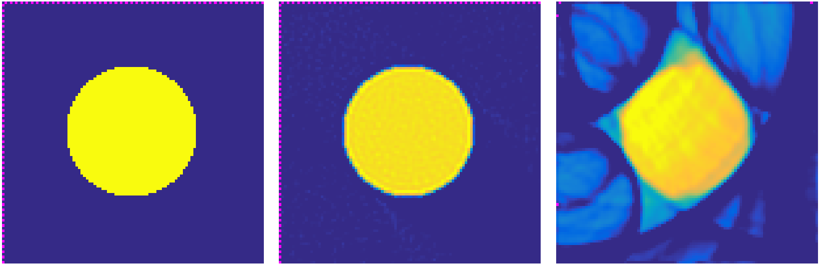

ground truth conventional data sub-sam. data

Better, but...

Iterative Least Squares with Non-Convex Projections

$$P^{k+1} = \Pi\left(P^k - \nu \nabla \tfrac{1}{2}\|CAP^k - F^c\|_2^2\right) = \Pi\left(P^k - \nu A^T C^T \left(CAP^k - F^c\right)\right)$$

- ✓ Π projection onto convex set, e.g., $\mathbb{R}_+^N$.
- ✓ Π proximal mapping for convex functional, e.g., nuclear norm, TV.
- ! Π projection onto non-convex set, e.g., non-negative matrix factorization.

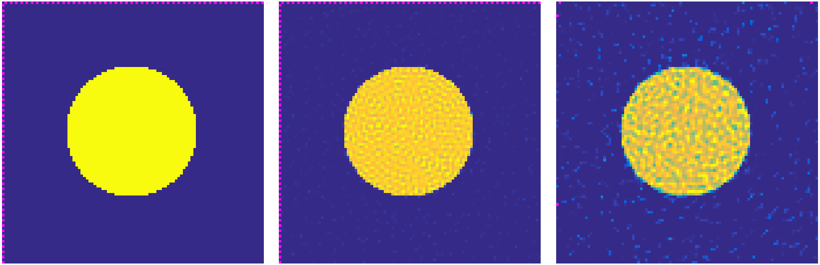

ground truth | conventional data | sub-sam. data

Recovers both geometry and spectrum!

Application: Quantitative PAT

Aim: Recover (relative) chromophore concentrations, e.g., blood oxygen saturation (sO_2).

Study: Recover known concentrations in tube phantom. PA reconstruction only first step in procedure.

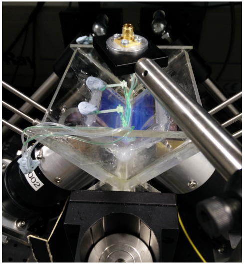

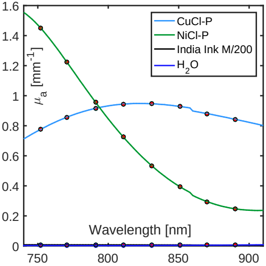

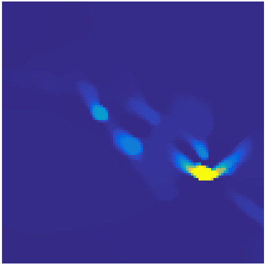

...but data is messy & computations are heavy, so no results yet **:/**

Joint ongoing struggle with Martina Bargeman Fonseca, Robert Ellwood, Emma Malone, Lu An, Ben Cox, Simon Arridge and Paul Beard.

Challenges of fast, high resolution 3D PA sensing:

- Nyquist requires several thousand detection points.
- Sequential schemes are slow.
- Crucial limitation for clinical, spectral and dynamical PAT.

Acceleration through sub-sampling:

- Exploit low spatio-temporal complexity to beat Nyquist.
- Acceleration by sub-sampling the incident wave field to maximize non-redundancy of data.
- Requires development of novel scanners.
- Demonstrated for Fabry-Pérot interferometer.

Results:

- Standard reconstruction methods fail on sub-sampled data.
- Adjoint PAT operator allows to use variational/iterative approaches.
- Sparse variational regularization/iterative non-convex projections give promising results for sub-sampled data.
- Demonstrated on simulated, experimental phantom and in-vivo data.

Challenges:

- Realizing this potential with experimental data requires
  - Model refinement/calibration.
  - Pre-processing to align data and model.
  - More suitable spatio-temporal constraints.
- High computational complexity.

- **Arridge, Beard, Betcke, Cox, Huynh, L, Ogunlade, Zhang, 2016**. *Accelerated High-Resolution Photoacoustic Tomography via Compressed Sensing*, *submitted, arXiv:1605.00133.*
- **Arridge, Betcke, Cox, L, Treeby, 2015**. *On the Adjoint Operator in Photoacoustic Tomography*, *submitted, arXiv:1602.02027.*

We gratefully acknowledge the support of NVIDIA Corporation with the donation of the Tesla K40 GPU used for this research.

Thank you for your attention!

- **Arridge, Beard, Betcke, Cox, Huynh, L, Ogunlade, Zhang, 2016**. *Accelerated High-Resolution Photoacoustic Tomography via Compressed Sensing*, *submitted, arXiv:1605.00133.*
- **Arridge, Betcke, Cox, L, Treeby, 2015**. *On the Adjoint Operator in Photoacoustic Tomography*, *submitted, arXiv:1602.02027.*

We gratefully acknowledge the support of NVIDIA Corporation with the donation of the Tesla K40 GPU used for this research.

Variational approaches,

$$\hat{p} = \operatorname*{argmin}_p \left\{ \tfrac{1}{2} \| CAp - f^c \|_2^2 + \lambda \mathcal{J}(p) \right\},$$

suffer from systematic bias (e.g., contrast loss for TV):

! Problem for quantitative use.

✓ Iterative enhancement trough Bregman iterations:

$$p^{k+1} = \operatorname*{argmin}_p \left\{ \frac{1}{2} \| CA\, p - (f^c + b^k) \|_2^2 + \lambda \mathcal{J}(p) \right\}$$
$$b^{k+1} = b^k + \left(f^c - CA\, p^{k+1} \right)$$

Potential for sub-sampling demonstrated in several other applications.

Osher, Burger, Goldfarb, Xu, Yin, 2006. *An iterative regularization method for total variation-based image restoration*, *Multiscale Modeling and Simulation*, 4(2):460-489.

Contrast Enhancement by Bregman Iterations

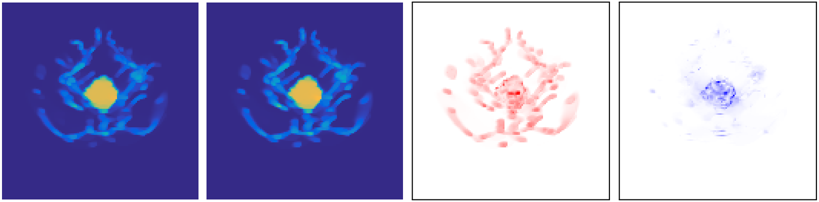

(a) TV+, cnv data (b) TV+Br, cnv data (c) $(p_{\text{TV+Br}} - p_{\text{TV+}})_+$, cnv data (d) $(p_{\text{TV+Br}} - p_{\text{TV+}})_-$, cnv data

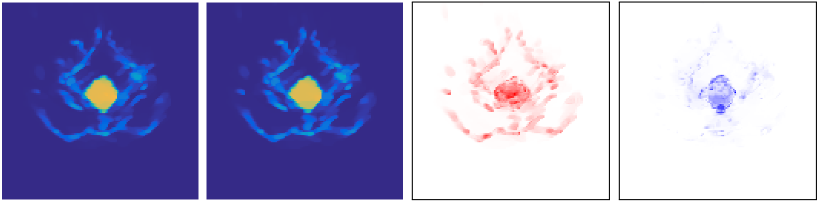

(e) TV+, rSP-128 (f) TV+Br, rSP-128 (g) $(p_{\text{TV+Br}} - p_{\text{TV+}})_+$, rSP-128 (h) $(p_{\text{TV+Br}} - p_{\text{TV+}})_-$, rSP-128

sensor on top; inverse crime data sampled at Nyquist; max intensity proj., side view

Iterative Schemes: Adjoint vs. Time Reversal

$$p^{k+1} = \Pi\left(p^k - \theta B\left(Ap^k - f\right)\right)$$

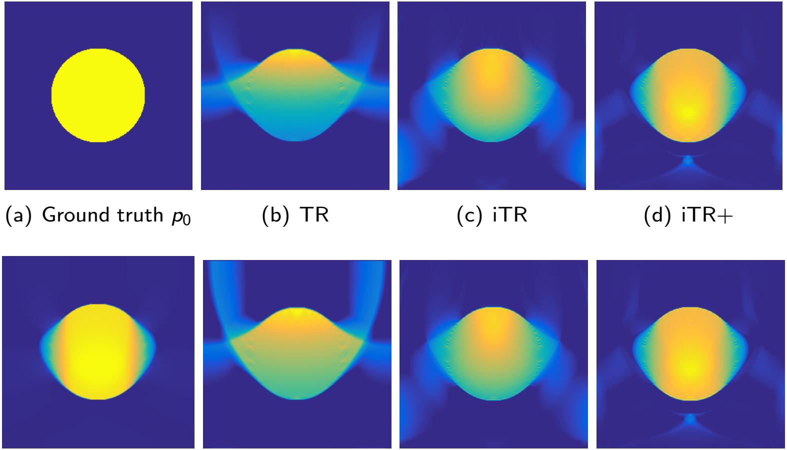

(a) Ground truth p_0 (b) TR (c) iTR (d) iTR+

(e) TV+ (f) BP (g) LS (h) LS+

sensor on top; 2D slices at $y = 128$ through the 3D reconstructions.

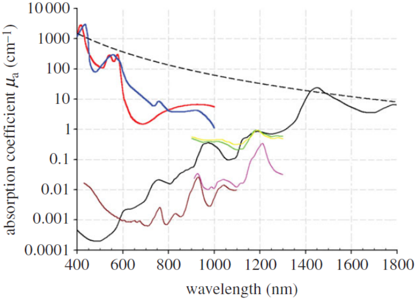

Figure 1. Absorption coefficient spectra of endogenous tissue chromophores. Oxyhaemoglobin (HbO_2), red line: (http://omlc.ogi.edu/spectra/hemoglobin/summary.html; 150 gl^{-1}), deoxyhaemoglobin (HHb), blue line: (http://omlc.ogi.edu/spectra/hemoglobin/summary.html; 150 gl^{-1}), water, black line [22] (80% by volume in tissue), lipid[a], brown line [23] (20% by volume in tissue), lipid[b], pink line [24], melanin, black dashed line (http://omlc.ogi.edu/spectra/melanin/mua.html; μ_a corresponds to that in skin). Collagen (green line) and elastin (yellow line) spectra from [24].

- High contrast between blood and water/lipid.
- Light-absorbing structures embedded in soft tissue.
- Gap between oxygenated and deoxygenated blood $\rightsquigarrow$ functional imaging.
- Different wavelengths allow quantitative spectroscopic examinations.
- Use of contrast agents for molecular imaging.

from: **Paul Beard, 2011**. *Biomedical photoacoustic imaging*, *Interface Focus.*

Nyquist Rates in Space and Time

- Up to now, conventional data was sampled at Nyquist rates in space and time (numerical phantoms were band-limited in space).
- In experiments, conventional data is usually already sub-sampled in space but over-sampled in time.
- Reconstruction on a finer spatial grid to exploit high frequency content of time series.

Example:

- Scan a 20mm×20mm with $\delta_x = 150\mu m$ (133×133 locations).
- Measured with temporal resolution of $\delta_t = 12$ns $\approx$ 83MHz.
- Low-pass filtered to 20MHz.
- Reconstructing a signal limited to 20MHz with a sound speed of $1540 \mathrm{m\,s^{-1}}$ would required $\delta_x = 38.5\mu m$ and $\delta_t = 25$ns.